Low-Power Detection of Sternocleidomastoid Muscle Contraction for Asthma Assessment and Control

Jun Luan, Seungjae Lee and Pai H. Chou
Center for Embedded Cyber-Physical Systems, University of California, Irvine, CA 92697-2625 USA
{jluan1, leesj3, phchou}@uci.edu

***Abstract*—Sternocleidomastoid (SCM) is a paired muscle that stretches along both sides of the neck area. It acts as an accessory muscle of inhalation. Abnormal SCM contraction during asthma is usually a sign of further respiratory impairment. Thus, monitoring SCM muscles has great significance in asthma assessment and control. In this work, we develop a wearable monitoring system based on an optical sensor that consists of an LED and a photo detector (PD). A voltage comparator enables the microcontroller unit (MCU) to remain in sleep mode until waken upon detecting contraction. Experimental results show that our optical sensor consumes much lower power than surface electromyography (sEMG), the most commonly used technique while offering more comfort and compactness. It is also robust to motion artifact and DC baseline wandering. These properties simplify the hardware design, while the use of the comparator further reduces the system power consumption to <450 μW on average, making it the best option for low power monitoring.**

***Keywords*—Optical sensor, Comparator, Sternocleidomastoid, Muscle contraction**

I. Introduction

SCM is a paired muscle that stretches along both sides of the neck area. When acting alone, it is in charge of head tilting and rotation. It is also involved in various neck movements and aids in forced inhalation when acting together with other muscles. Monitoring SCM muscle contraction is of great significance to asthma assessment and control. Abnormal SCM contraction during asthma is usually a sign of further respiratory impairment. SCM retraction happens in 40% of the asthma episodes [1], and SCM contraction associated with asthma usually indicates a more severe disease in children [2].

The motivation of this work is to design a long-term wearable monitoring device to detect and record SCM contraction events during an asthma attack. The recorded data will be later assessed by physicians to make a treatment plan. Low power consumption is essential for battery life and therefore longer monitoring time, as well as wearing comfort due to the size and weight of the battery. However, the SCM contraction is sporadic and fast. The duration of the contraction can be as short as 24 ms [3]. The traditional uniform sampling scheme cannot solve this problem since it takes full power for the MCU to sample and process the signal at such a high rate.

In this work, we design a novel system that utilizes an optical sensor, which consists of an LED and a PD, and a voltage comparator that enables the MCU to stay in low-power mode and wakes it up when contraction signal detected. To simplify the hardware structure, the brightness of the LED can be controlled by MCU's pulse width modulator (PWM). A two-phase algorithm, learning and detecting, is also designed to detect the muscle contraction. In the learning phase, the LED brightness level is swept to determine the best PWM duty that controls the input signal under the desired threshold. In the detecting phase, the processed signal from the PD is compared with the comparator reference. Only when it exceeds the reference will the MCU be awakened from low-power mode to detect the signal peak and count the times of the contraction using a threshold-based algorithm. The contribution of this work lies in the novelty of the system design and the lower-power control of the optical sensor.

Because SCM is in the superficial layer of the neck, options capable of detecting muscle movements inlcude sEMG, the accelerometer and the optical sensor. Among them, sEMG is most mature technology for this purpose and can capture high quality signal [4], but its drawbacks include bulkiness, discomfort and power consumption.

To select the most suitable sensor, we conducted a comparative study among all three types of sensors. This study shows the optical sensor to be the best among the three for low-power monitoring of muscle activities. With proper control of the LED brightness, the optical sensor can consume much less power than sEMG, while the hardware design is more compact and more comfortable to wear. Even though the signal-to-noise ratio (SNR) of the optical signal is lower than that of sEMG, the optical signal is more stable with little baseline wandering. This feature simplifies the system structure and facilitates the use of a comparator, which further reduces the power consumption.

This paper first provides a background on optical sensors and sEMG. We describe our proposed sensor system and detection algorithm. We evaluate it by comparing it with two other types of sensing modalities. The experimental results are analyzed with a discussion of the implications.

II. Background And Related Works

EMG measures the action potential generated by muscle fiber contraction, while sEMG replaces the needle type with the non-invasive surface-type electrode, which is more comfortable to wear. One significant drawback of sEMG is the power consumption. The state-of-the-art sEMG uses the precision instrumentation amplifier (in-amp) [5]. The in-amp is a special type of differential amplifier that adopts an input buffer to ease the impedance matching with the preceding stage. In-amps with low noise, low offset, and low drift are classified as precision in-amps. Commercially available precision in-amps consume milliwatts of power as shown in Table I. Another drawback is the bulkiness of the system due to the use of electrodes. Many applications require a minimum of three, two of which on the target muscle to measure the differential signal and a third ground electrode serving as the reference point for the precision in-amp. This ground electrode should be put on a bony or non-muscular part of

the body as far as possible from the target muscle in order to generate a stable reference. Special design is available [6], but commercial electrodes are usually over 20 mm in diameter. A third drawback is that an extra step of skin preparation is needed to get good signal quality. The purpose of skin preparation is to add moisture between the skin surface and the electrode to increase the input impedance of the in-amp. The general procedure includes cleaning and rubbing the skin, hair removal, and applying conductive gel for better contact. In fact, pre-gelled electrodes are the most often used in sEMG [7], but the gel can cause skin reaction and drying over time, making it less suitable for long-time monitoring.

The optical sensor requires no skin preparation and can be comfortably worn as long as it is put close enough to the skin surface. It utilizes one or multiple LEDs to emit light into human tissues and one or multiple PDs to measure the transmittance or reflectance of the light. The optical sensor has been widely used in pulse oximetry to obtain photoplethysmogram (PPG) [8]. Many health-critical biophysical indices can be extracted from PPG, such as heart rate, blood oxygen concentration (SpO2), respiration rate, and more. An optical probe can be potentially made in tiny size using a miniaturized LED-PD combo chip [9].

Using optical sensors to monitor muscle activity is a relatively new research area. It is shown in [10] that near infrared (NIR) spectroscopy can be used to detect isometric and isokinetic muscle contractions. Wearable optical sensors are developed in [11]–[13] to activate prosthetic limbs. These works, however, only focus on the function side of the optical sensors, but power consumption and power saving techniques have not been addressed.

Traditionally, active optical devices are considered high power consumption because of the LED. Pulse oximeters usually consumes 55-120 mW, most of which is by the LED [14]. To reduce power for long-term monitoring, some researchers resort to compressive sensing to decrease the sampling rate [15], [16]. Compressive sensing, however, is not suitable for this purpose, because it usually requires a powerful back-end computing unit to perform signal reconstruction [17] and the system often suffers from the subsequent delay. In this work, we design a low-power standalone device with real-time performance. We show that by careful selection and control of the sensor, the power consumption can be optimized without complicated high-level techniques.

III. Technical Approach

This section first provides the usage requirements, followed by a description of the hardware system and the detection algorithm.

A. Usage Requirements

The optical sensor is placed on top of the sternal head of left SCM muscle inside the anterior cervical triangle [18], close to the clavicle as shown in Fig. 1a. On this location, the greatest signal strength of voluntary contraction can be sensed while the respiratory signal noise is suppressed at a tolerable level. If the sensor is moved more to the left side, the contraction signal becomes weaker. If moved to the right side, the respiratory noise increases.

B. Hardware System

Fig. 2 shows the block diagram of the proposed low-power reflective optical sensing system for SCM contraction.

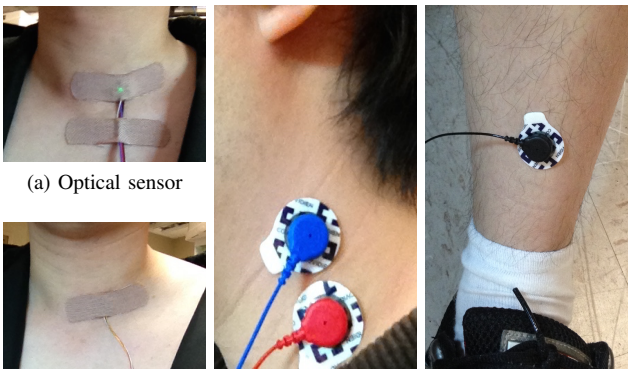

(a) Optical sensor (b) Accelerometer (c) sEMG: neck electrodes (d) sEMG: leg electrode

Fig. 1: Placement of sensors for testing muscle contraction.

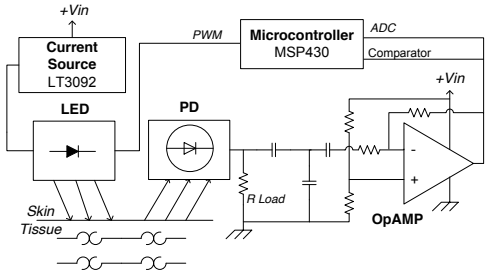

Fig. 2: Proposed optical system

It consists of a light emitter with a current source, a PD with an OpAMP, and an MCU.

1) Light Emitter: The light emitter subsystem consists of a PWM-controlled LED (AM2520ZGC09) driven by a current source (LT3092) [19]. We choose the green LED with the peak wavelength of 515 nm that is proved to be more robust to motion artifact than red or blue in the applications of heart rate and pulse volume detection [20]. The current from the LED is sinked into the PWM controller for brightness control.

Fig. 3 shows the optical sensor board. It may appear bulky, but actually the system can be further miniaturized. The LED on-time is set to approximately 200 μs in every 16 ms by PWM control. Fast switching of LED causes the current surge due to the change of LED forward voltage. To suppress the inrush current, we use the current source to drive the LED.

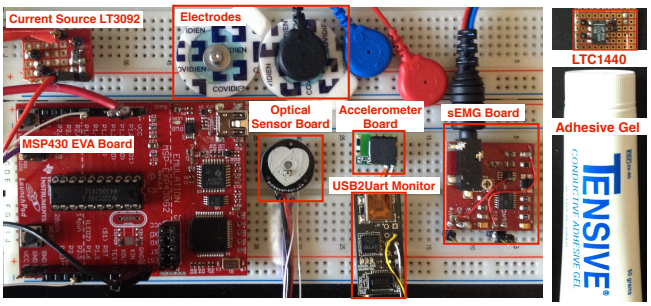

Fig. 3: Hardware prototype

The driving current is fixed to 500 μA.

2) Photo Detector and OpAMP: The PD (APDS-9008) is chosen based on its peak response wavelength matching the LED wavelength. This will achieve the highest efficiency and therefore power minimization. The PD outputs a current signal that is then transformed into a voltage signal by the load resistor. The voltage signal is further filtered by a low pass filter (LPF) and amplified by the OpAMP (MCP6001).

3) Voltage Comparator: The voltage comparator enables the MCU to sleep without sampling the signal and wakes it up by interrupt upon detecting muscle contraction based on the intensity of the optical signal. The on-chip comparator of our MCU (MSP430) [21] is used and a reference voltage of $\frac{1}{2}V_{cc}$ is applied to the comparator minus input. As shown in Fig. 4a, when the amplified PD signal exceeds the reference voltage, the comparator wakes up the MCU.

The power overhead of the comparator is 45 μA in active mode and can be reduced by duty cycling. Two interrupt service routines (ISR) are set on the falling and rising edges of PWM to switch the comparator on and off, respectively. The on-time is very short, and the timing of these routines are shown by a test pin in the same figure. In the real system, the MCU will immediately turn off the comparator upon wake-up by the comparator trigger and also disable the off routine.

An external comparator LTC1440 [22] is also added to the system used in the comparative study. The reference voltage of LTC1440 is fixed to $\frac{1}{2}V_{cc}$ by a voltage divider. This voltage is set higher than the highest respiration peak in order to prevent false trigging. By adding this comparator, the MCU can remain in sleep mode most of time, including walking, sitting, and sleeping. LTC1440 consumes under 4 μA in active mode.

4) Microcontroller Unit: We use an MSP430 as the low-power MCU, although just about any MCU can be used. The MCU will stay in low-power mode 3 (LPM3, the lowest-power sleep mode, at 0.5 μA) waiting to be triggered. Once triggered by the comparator, the MCU will enter continuous-sampling mode by setting a timer interrupt to the falling edge (i.e. LED-on edge) of the PWM signal. The amplified PD signal is sampled by a 10-bit ADC every 16 ms, and the samples are further processed to detect SCM contraction as discussed in Section III-C. Once the SCM contraction is no longer detected, the MCU will disable the timer interrupt, reactivate the comparator, and go back to LPM3.

Fast switching of the optical sensor is made easier with the built-in PWM generator. The LED on-time can be easily set and changed by setting the duty. The clock of PWM is sourced to auxiliary clock (ACLK), which is still functioning in LPM3. Delay effect of the LPF can be seen on Fig. 4b. To overcome this delay, the signal is sampled 3 times in around 100 μs interval and only the maximum value is taken. We also explored the option to switch off OpAMP periodically but the system suffers from the severe delay caused by the LPF and OpAMP during fast switching. We ended up leaving the OpAMP on all the time instead of duty cycling it.

C. Detection Algorithm

The detection algorithm can be summarized as a two-phase learning one that adapts the LED brightness based on the signal peak. The main reason for learning is that the peak level of SCM contraction varies among people. For example, adults are supposed to generate stronger contraction than youngsters. Neck or head movement can also trigger the interrupt as shown in Fig. 9 Fig. 10. Such repetitive movements can be falsely detected as the SCM contraction. This is still tolerable since the recorded signal is supposed to be analyzed in parallel with other data such as stethoscope recordings [23] by physicians.

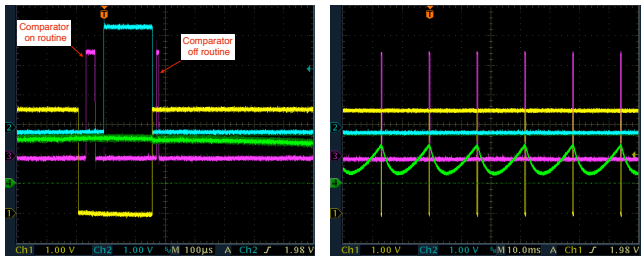

(a) Interrupt triggered (b) No trigger signal

Fig. 4: Optical Sensor with comparator control. Yellow, PWM LED control, blue: comparator trigger, pink: comparator on and off ISRs, green: amplified PD output

The designed algorithm, as shown in Algorithm 1, increases the coverage of our system. In the learning stage, the patient is asked to breathe normally. The device will scan the LED brightness by setting the PWM duty. In each duty level, the MCU simply detects the maximum peak of the signal for 5 s. The duty with the signal peak closest to but below the threshold is used in the next stage. A threshold-based algorithm is implemented to count the peaks. As shown in Section IV, the signal generated by the optical sensor is robust to motion artifact and free from baseline wandering. This simple threshold based algorithm works well enough to detect the contraction.

Input: current signal sample: *current_sample*, sample data buffer: *data_buf*, detecting mode: *detect_mode*
Output: contraction flag: *contrc_flag*
learning
  while *max_sample* < LO_THD **do**
    SAMPLE_SIGNAL(*data_buf*)
    max_sample ← MAXIMUM(*data_buf*)
    SET_PWM_DUTY(++*pwm_duty*); */* raise exception if out of the range and redo learning */*
  end
  SET_PWM_DUTY(−−*pwm_duty*)
  SET_DEC_MODE(DETECTING)
end
detecting
  if *current_sample* ≥HI_THD **and** *first_peak* == FALSE **then**
    first_peak ← TRUE; */* first peak can also be set in the comparator ISR */*
  else if *current_sample* < HI_THD **and** *first_peak* == TRUE **then**
    peak_count++
    first_peak = FALSE
  else if *current_sample* ≥ HI_THD **and** *first_peak* == TRUE **then**
    if ++*peak_timer* > PEAK_LIMIT **then**
      MODE_RESET()
    end
  else if *current_sample* < HI_THD **and** *first_peak* == FALSE **then**
    if ++*valley_timer* > VALLEY_LIMIT **then**
      MODE_RESET()
    end
  end
  if *peak_count* > 2 **then**
    return TRUE
  end
  return FALSE
end

Algorithm 1: SCM Contraction Detection Algorithm

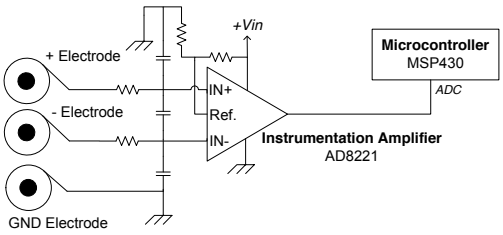

(a) Surface EMG system

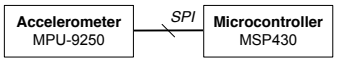

(b) Accelerometer system

Fig. 5: Other Sensing Modalities for Muscle Contraction Monitoring

IV. Evaluation

To evaluate our muscle tension sensor, we compare the results with different sensing modalities for their power consumption and signal quality. Power consumption varies with the details of the hardware and software design. We consider not only power at the component level, but also the complexity of the software algorithm, which directly affects the energy consumption. The signal quality of the sensor also has an impact since more processing may be required to recover the key component of interest.

To make our comparison fair and practical, we stick to the specific purpose of monitoring SCM contraction rather than general muscle movements. We also use commercially available components rather than custom designs for this purpose. We evaluate the power consumption as the primary objective and accurate detection of contraction in real time as the secondary, rather than pursuing the best noiseless signal.

A. Comparative Systems

For fast prototyping of the system, we use the pulse sensor board in [24] for the optical sensor and muscle sensor board in [25] for sEMG. We adapted both boards for our comparison as shown in Fig. 5. We use an MSP430G2452 [21] evaluation board as the MCU board for sEMG and the optical sensor with the MCU running at 1 MHz on a 3.3 V power supply. For the accelerometer, we designed a prototype using TI's CC2541 Bluetooth Low Energy (BLE) single-chip MCU [26] to control the MPU-9250 accelerometer [27]. A UART monitor is used to transfer the signal to a computer. All the hardware used in this study is shown in Fig. 3. The sampling rate is set to 62.5 Hz (16 ms period) as a representative number. The same contraction detecting algorithm is running on the MCUs for all sensors. It is a simple threshold-based algorithm doing sample-by-sample analysis described in Section III-C.

1) Accelerometer: The system is shown in Fig. 5b. The sensor is placed in the same spot as the optical sensor as shown in Fig. 2. MPU-9250 is a low-power 9 degree-of-freedom (9-DoF) inertial sensor with a triaxial accelerometer, gyroscope, and compass. It is controlled by the SPI interface of the CC2541 MCU. Acceleration data is sent out from the MCU through UART interface. The size of whole system including CC2541 is only 12 mm$\times$ 9 mm, making it highly wearable.

2) Surface EMG: A two-stage design consisting of an instrumentation amplifier plus OpAMP is common for sEMG.

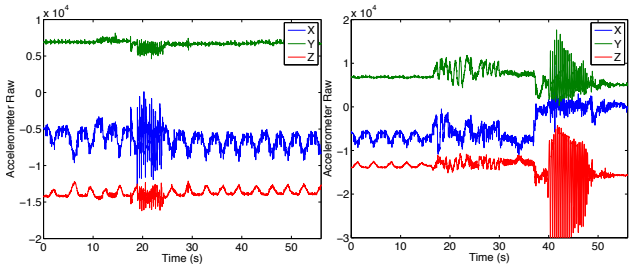

(a) Still state (b) Light to moderate movement

Fig. 6: Voluntary contraction signal from accelerometer

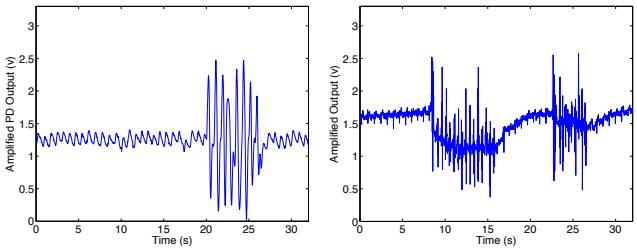

(a) Optical sensor (b) sEMG

Fig. 7: Voluntary contraction

The in-amp serves as a pre-amplifier, rejecting the common mode noise and amplifying the signal only with a small gain. The second stage further amplifies the signal and is usually built in with strong filters to deal with motion artifact and baseline wandering. To simplify the circuitry, we remove the second stage amplifier while increase the gain in the first stage. This inevitably reduces the signal amplitude but saves power.

B. Signal Quality

1) Accelerometer: When the body is in a still state, voluntary contraction can be easily seen. However, SCM muscle contraction cannot be detected during body movement. The signals of voluntary contraction during body movements are shown in Fig. 6. It is extremely difficult to detect the contraction even under light upper body movement such as walking and jogging, while these movements are common in daily life.

2) Surface EMG vs. Optical: Figs.7-10 compare the sEMG signals with those from the optical sensor over different scenarios. sEMG generates better signal in term of amplitude and SNR. The in-amp of the sEMG can also remove body noise

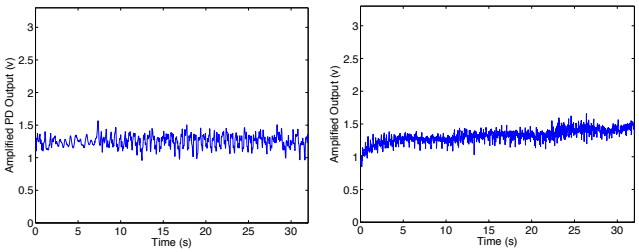

(a) Optical sensor (b) sEMG

Fig. 8: Jogging with no neck movement

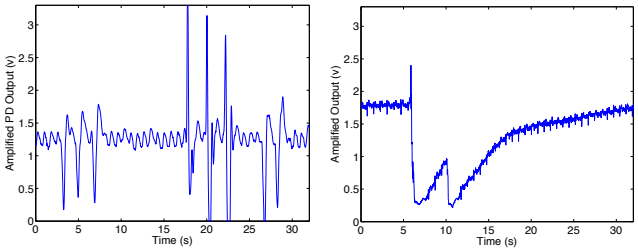

(a) Optical sensor (b) sEMG

Fig. 9: Turning right and then left

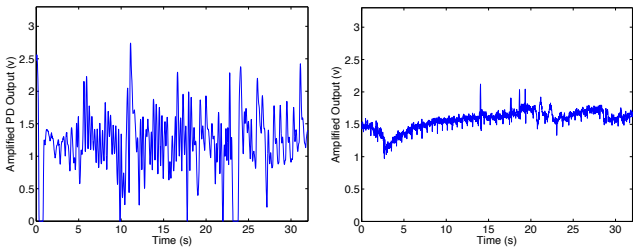

(a) Optical sensor (b) sEMG

Fig. 10: Continuous head up and down

such as electrocadiac and respiratory signals very well compared to the optical sensor. However, great baseline wandering can be observed from the graph. Under this influence, the simple thresholding algorithm does not work well on sEMG. Further hardware or software filtering is definitely needed to remove it. For the optical sensor, clear respiratory cycles can be seen in the signal in Fig. 7a, but the optical signal is more stable with little changing to the baseline. Similar to sEMG, most of the moderate movements such as walking and jogging do not necessarily cause motion artifact unless the neck area moves. Among all the movements, right turn triggers the greatest peak. Lifting the head up and down generates similar signal peaks to voluntary contraction.

We realized from this study that sEMG is not suitable for this application for two main reasons. First is the use of adhesive gel. The signal changes over time due to the drying of the gel that changes the skin-electrode impedance. The other is that a third ground electrode is critical to the signal and has to be put far away to generate a stable reference. These constraints inevitably increase the discomfort level and inconvenience to the patient's daily life.

C. Power Consumption

1) Accelerometer: The current consumption of MPU-9250 is just 19.8 μA in active accelerometer mode and 8 μA in standby mode. Unfortunately, as shown in Section IV-B1, the MPU-9250 is too susceptible to body movement for this application, even though it would otherwise be perfect in terms of power consumption and wearing comfort.

2) Surface EMG vs. Optical: The dominant power consumer in sEMG is the precision in-amp. AD8221 [28] is used in our sEMG design. Table I compares it with some other commercially available products that basically have the same function set. It shows that AD8221 is one of the best among the list with a relatively low supply current but good performance

TABLE I: Commercial Precision Instrumentation Amplifiers

P. N.	AD8221	AD624	INA326	LTC2053	LT1167	MAX4208
Supply Current	0.9mA	2.5mA	2.4mA	0.75mA	1.3mA	0.75mA
Gain	$1-10^3$	$1-10^3$	$0.1-10^4$	$1-10^3$	$1-10^4$	100
Bandwidth (0.1-10Hz)	825kHz	25MHz	1kHz	200kHz	200kHz	750kHz
Input Noise ($\mu VP-P$)	0.25	0.2	0.8	2.5	0.28	2.5
CMRR DC G=1	90dB	80dB	70dB	116dB	86dB	135dB
CMRR 10kHz G=1	80dB	40dB	70dB	¡100dB	62dB	120dB

in term of noise and bandwidth. There are also so-called micropower precision in-amps that consume only hundreds of microwatts, but they are usually optimized for very low input stage current [5]. Thus, the noise level is usually higher than the higher current amplifiers shown in Table I.

Frequent switching of in-amp is not an option for power saving. Power supply should be turned on before the input signal to avoid overloading the amplifier. In the case of AD8221, once the output voltage goes beyond the supply rails, the protection diodes will be turned on. Even if the in-amp is not damaged, significant noise and delay might occur due the fast switching. As a result, we keep the AD8221 on all the time. A 16-ms timer is set to wake up the MSP430 from LPM3 and sample the signal. The ISR duration and the in-amp output signal are shown on Fig. 11b. An MCU port is pulled up at the beginning and pulled down at the end of the interrupt. The duration of the ISR varies depending on the input signal and the stage of signal processing. For the optical sensor, the interrupt is set on the falling edge of PWM to sample the signal without activating the comparator. This is shown in Fig. 11c with the current signal from the power supply.

The power consumption is compared by attaching sEMG to one side of the SCM muscle and the optical sensor to the other. In this way, approximately the same input signal can be generated by the symmetric left and right movements. The current signal is monitored and recorded using an oscilloscope. The data is very noisy as shown in Fig. 11, and current consumption is mostly in the form of surge current due to the charging and discharging of the capacitive components in the circuit. We are able to calculate the average power by doing integral. For sEMG, the average current during the ISR is 2578 μA and a current of over 2 mA is constantly drawn by the in-amp with an average power of over 6.6 mW. The ISR duration is measured as from 170 μs to 280 μs. For the optical sensor, the average current consumption from LED on to the end of the ISR is calculated as 589 μA with the duration varies from 320 μs to 540 μs. Even though the duration is much longer than sEMG because of the sampling interval, the average power consumption in a 16 ms cycle is only around 450 μW. The current probe definitely introduces large error in measuring the noisy sub-mA current, but the comparison clearly shows that sEMG consumes much more current than the optical sensor does.

V. Conclusions

In this paper, we have presented a low-power, compact, optical sensor system for detection of sternocleidomastoid muscle contraction. We compared common sensing modalities,

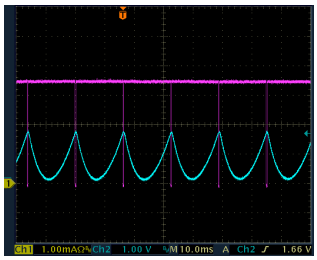

(a) Optical sensor interrupt. Pink: PWM, blue: amplified PD output

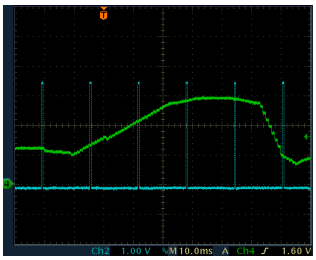

(b) sEMG interrupt. Blue: interrupt flag, green: in-amp output

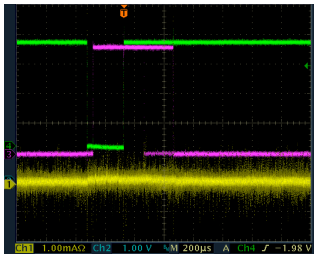

(c) Optical sensor current consumption. Yellow: system current (mA), pink: interrupt flag, green: PWM

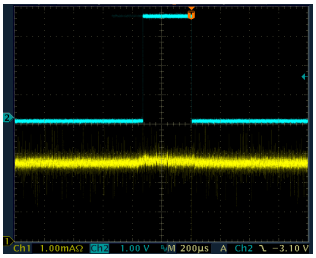

(d) sEMG current consumption. Yellow: system current (mA), blue: interrupt flag

Fig. 11: Signal comparison between optical sensor and sEMG

including accelerometry and surface electromyography, and we showed the optical one to be the most suitable by striking the best balance among the size, power, and sensitivity. In addition to the hardware, we also describe the detection algorithm that handles variations ranging from adults to young children. Together, our hardware and software techniques will enable a new generation of highly wearable monitors for precise monitoring of asthma symptoms and other respiratory diseases. This is currently an important area with sorely unmet need for wearable monitors.

Acknowledgments

This work was sponsored by the National Institute of Health (NIH) STTR Phase II Grant 2R42HL112435-03 through a subcontract by QT Medical, Inc. The content is solely the responsibility of the authors and does not necessarily represent the official views of the sponsors.

REFERENCES

[1] S. G. Kelsen, D. P. Kelsen, B. F. Fleeger, R. C. Jones, and T. Rodman, "Emergency room assessment and treatment of patients with acute asthma. adequacy of the conventional approach." *Am J Med*, vol. 64, no. 4, pp. 622–628, Apr 1978.

[2] J. O. Commey and H. Levison, "Physical signs in childhood asthma." *Pediatrics*, vol. 58, no. 4, pp. 537–541, Oct 1976.

[3] I. Stockman, "Neck muscle influence in rear impacts–a sled test study using the BioRID," 2010.

[4] M. Mananas, J. Fiz, J. Morera, and P. Caminal, "Analyzing dynamic EMG and VMG signals of respiratory muscles," *Engineering in Medicine and Biology Magazine, IEEE*, vol. 20, no. 6, pp. 125–132, Nov 2001.

[5] L. Couts, "A designer's guide to instrumentation amplifiers. chap. 1," 2006.

[6] E. Vavrinsky, M. Daricek, M. Donoval, K. Rendek, F. Horinek, M. Horniak, and D. Donoval, "Design of EMG wireless sensor system," in *Applied Electronics (AE), 2011 International Conference on*, Sept 2011, pp. 1–4.

[7] P. Konrad, "The ABC of EMG," *A practical introduction to kinesiological electromyography*, vol. 1, 2005.

[8] T. Rusch, R. Sankar, and J. Scharf, "Signal processing methods for pulse oximetry," *Computers in Biology and Medicine*, vol. 26, no. 2, pp. 143 – 159, 1996. [Online]. Available: http://www.sciencedirect.com/science/article/pii/0010482595000496

[9] "COBP Photo Reflector with RED and IR LED," http://www.njr.com/semicon/products/NJL5501R.html.

[10] A. Gelmetti, M. E. Giardini, P. Lago, R. Pavesi, D. Zambarbieri, R. Maestri, and G. Felicetti, "Preliminary study of muscle contraction assessment by nir spectroscopy," pp. 61–67, 1998. [Online]. Available: http://dx.doi.org/10.1117/12.301108

[11] A. K. Bansal, S. Hou, O. Kulyk, E. M. Bowman, and I. D. W. Samuel, "Wearable organic optoelectronic sensors for medicine," *Advanced Materials*, pp. n/a–n/a, 2014. [Online]. Available: http://dx.doi.org/10.1002/adma.201403560

[12] H. Han and J. Kim, "Novel muscle activation sensors for estimating of upper limb motion intention," in *Engineering in Medicine and Biology Society, 2009. EMBC 2009. Annual International Conference of the IEEE*, Sept 2009, pp. 3767–3770.

[13] T. Bianchi, D. Zambarbieri, G. Beltrami, and G. Verni, "NIRS monitoring of muscle contraction to control a prosthetic device," pp. 157–163, 1999. [Online]. Available: http://dx.doi.org/10.1117/12.336926

[14] M. Tavakoli, L. Turicchia, and R. Sarpeshkar, "An ultra-low-power pulse oximeter implemented with an energy-efficient transimpedance amplifier," *Biomedical Circuits and Systems, IEEE Transactions on*, vol. 4, no. 1, pp. 27–38, Feb 2010.

[15] P. K. Baheti, H. Garudadri, and S. Majumdar, "Blood oxygen estimation from compressively sensed photoplethysmograph," in *Wireless Health 2010*, ser. WH '10. New York, NY, USA: ACM, 2010, pp. 10–14. [Online]. Available: http://doi.acm.org/10.1145/1921081.1921084

[16] P. K. Baheti and H. Garudadri, "Heart rate and blood pressure estimation from compressively sensed photoplethysmograph." ICST, 5 2010.

[17] E. Candes, J. Romberg, and T. Tao, "Robust uncertainty principles: exact signal reconstruction from highly incomplete frequency information," *Information Theory, IEEE Transactions on*, vol. 52, no. 2, pp. 489–509, Feb 2006.

[18] M. Grodinsky and E. A. Holyoke, "The fasciae and fascial spaces of the head, neck and adjacent regions," *American Journal of Anatomy*, vol. 63, no. 3, pp. 367–408, 1938. [Online]. Available: http://dx.doi.org/10.1002/aja.1000630303

[19] "Programmable Current Source LT3092," http://www.linear.com/product/LT3092.

[20] K. Matsumura, P. Rolfe, J. Lee, and T. Yamakoshi, "iPhone 4s photoplethysmography: Which light color yields the most accurate heart rate and normalized pulse volume using the iPhysioMeter application in the presence of motion artifact?" *PLoS ONE*, vol. 9, no. 3, p. e91205, 03 2014. [Online]. Available: http://dx.doi.org/10.1371%2Fjournal.pone.0091205

[21] "Ultra-low-power microcontrollers MSP430," http://www.ti.com/product/msp430g2452?keyMatch=msp430g2452&tisearch=Search-EN-Everything.

[22] "Ultralow Power Comparator LTC1440," http://www.linear.com/product/LTC1440.

[23] A. Homs-Corbera, J. Fiz, J. Morera, and R. Jane, "Time-frequency detection and analysis of wheezes during forced exhalation," *Biomedical Engineering, IEEE Transactions on*, vol. 51, no. 1, pp. 182–186, Jan 2004.

[24] "Pulse Sensor," http://pulsesensor.com.

[25] "Muscle Sensor v3," http://www.advancertechnologies.com/p/muscle-sensor-v3.html.

[26] "CC2541 SimpleLink Bluetooth Smart and Proprietary Wireless MCU," http://www.ti.com/product/cc2541.

[27] "MPU9250 Motion Sensor," http://www.invensense.com/mems/gyro/mpu9250.html.

[28] "Low Power Instrumentation Amplifer," http://www.analog.com/en/products/amplifiers/instrumentation-amplifiers/ad8221.html.